

# RSC Advances



This article can be cited before page numbers have been issued, to do this please use: P. Salvatori, S. Agrawal, C. Barredden, C. Malapaka, M. de Borniol and F. De Angelis, *RSC Adv.*, 2014, DOI: 10.1039/C4RA09472G.



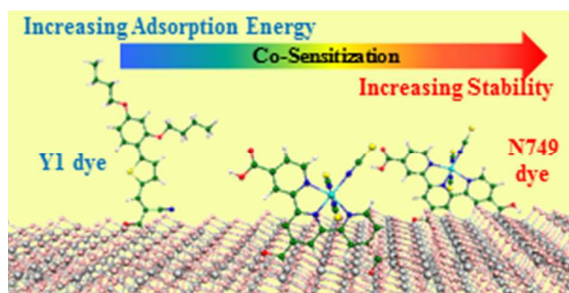
This is an *Accepted Manuscript*, which has been through the Royal Society of Chemistry peer review process and has been accepted for publication.

*Accepted Manuscripts* are published online shortly after acceptance, before technical editing, formatting and proof reading. Using this free service, authors can make their results available to the community, in citable form, before we publish the edited article. This *Accepted Manuscript* will be replaced by the edited, formatted and paginated article as soon as this is available.

You can find more information about *Accepted Manuscripts* in the [Information for Authors](#).

Please note that technical editing may introduce minor changes to the text and/or graphics, which may alter content. The journal's standard [Terms & Conditions](#) and the [Ethical guidelines](#) still apply. In no event shall the Royal Society of Chemistry be held responsible for any errors or omissions in this *Accepted Manuscript* or any consequences arising from the use of any information it contains.

## Table of contents



Higher stability for the N749 and N749/Y1 co-sensitized devices compared to Y1 based ones. DFT calculations show lower adsorption energy for Y1, that could be desorbed.

## ARTICLE

# Stability of ruthenium/organic dye co-sensitized solar cells: a joint experimental and computational investigation.

Cite this: DOI: 10.1039/x0xx00000x

Received 00th January 2012,  
Accepted 00th January 2012

DOI: 10.1039/x0xx00000x

www.rsc.org/

Paolo Salvatori,<sup>a,b\*</sup> Saurabh Agrawal,<sup>b</sup> Chiranjeevi Barreddi,<sup>c</sup> Chandrasekharam Malapaka,<sup>c</sup> Mervyn de Borniol,<sup>d</sup> Filippo De Angelis,<sup>b\*</sup>

A joint experimental and theoretical study on the stability of dye-sensitized Solar Cells employing a mixture of black dye (N749) and Y1 organic coadsorbent is presented. The aim of the present work is to investigate the stability of these sensitizers, representing the efficiency state of the art in this field. Under the investigated conditions (1100h of ~1Sun light soaking at 55°C) the co-sensitized device has shown a remarkable stability. The partial desorption of the organic co-adsorbent has been individuated as a possible cause for the slight reduction of the photocurrent value. Theoretical investigations through DFT methods on the dye-sensitized semiconductor surface, revealed a considerably lower adsorption energy for Y1 compared to N749, in particular upon oxidation, possibly leading to the dye desorption under working conditions. Coherently, devices employing only the Y1 organic dye have shown a considerably lower durability.

## 1 Introduction

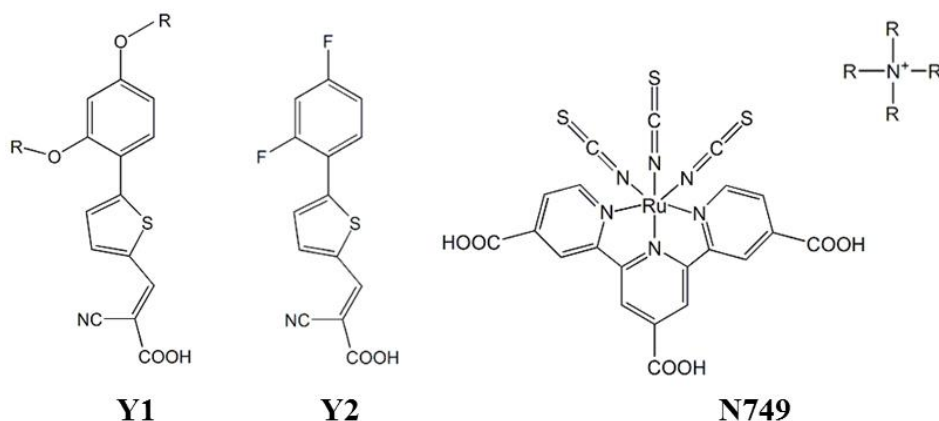
Constant depletion of our natural resources coupled with environmental concerns has fuelled the necessity to develop efficient alternative energy technologies. Among these, photovoltaic devices, ensuring direct conversion of visible light to electrical power have recently represented a viable solution. Dye-sensitized Solar Cell (DSC) technology is one of the emergent photovoltaic technologies,<sup>1-4</sup> with highest reported efficiencies of 13% to date.<sup>5</sup> Besides the high efficiencies, long term stability is another clear requirement toward the possible commercialization of this technology.

A standard DSC comprises a wide band gap titanium dioxide (TiO<sub>2</sub>) metal oxide layer sintered over a transparent conducting fluorine-doped tin oxide (FTO) electrode. A monolayer of photoactive dye is adsorbed on the nanocrystalline TiO<sub>2</sub> surface. A redox shuttle (I<sup>-</sup>/I<sub>3</sub><sup>-</sup> or Co(II)/Co(III) complex) solution fills the interstitial space between the sensitized semiconductor and a platinized counter-electrode. In these cells, the photo-excited dye transfers an electron to the TiO<sub>2</sub> conduction band and the oxidized dye is then reduced by the redox mediator in the electrolyte. The injected electrons percolate through the metal oxide network, reach the FTO electrode and are transferred to the platinized counter-electrode through the external circuit. At the counter-electrode the electrons regenerate the redox shuttle and close the circuit. In DSC devices, dyes play a critical role in determining efficient

charge generation and separation at the interface with the semiconductor. Ruthenium-based dyes,<sup>6-8</sup> porphyrin dyes,<sup>9-12</sup> and organic dyes<sup>13, 14</sup> are the most investigated classes of sensitizers in this field.

Light absorption in the visible and near infra-red (IR) part of the solar spectrum is a key requirement of a DSC sensitizer. Besides the dye structure engineering, in order to enhance the spectral response in the near IR region, co-sensitization by multiple dyes, having complementary light absorption, has been explored.<sup>15-18</sup> A peculiar application of co-sensitization has been reported by Han and coworkers in 2012.<sup>19</sup> In order to outweigh the competitive light absorption by I<sup>-</sup>/I<sub>3</sub><sup>-</sup> electrolytes,<sup>20</sup> they co-adsorbed the Y1 organic dye (Scheme 1), having a strong absorption at 400 nm, with the panchromatic [Ru(H<sub>3</sub>tcterpy)(NCS)<sub>3</sub>] (tcterpy=4,4',4''-tricarboxy-2,2':6',2''-terpyridine), well known as N749 or black dye (Scheme 1), resulting in an improved certified efficiency of 11.4%.<sup>19</sup>

Another important requisite of a sensitizing dye is the grafting capability at the semiconductor surface. Three fundamental properties essentially depend on the anchoring moieties: (i) the electronic coupling between the dye and the metal oxide, and then the charge injection efficiency,<sup>21, 22</sup> (ii) the orientation and the packing of the adsorbed dyes, influencing the recombination processes,<sup>23, 24</sup> and finally (iii) the long-term stability of the device.<sup>25, 26</sup>



**Scheme 1.** Chemical structures of (a) Y1 dye, (b) Y2 dye, (c) N749 dye, with the tetrabutylammonium (TBA) counterion. Here R= C<sub>4</sub>H<sub>9</sub>.

For these reasons, the binding behaviour of the sensitizer on anatase TiO<sub>2</sub> surface has been deeply investigated. For an organic dye, generally bearing one carboxylic acid, the most employed anchoring group, the commonly accepted picture extracted by FT-IR analysis and theoretical calculations is that the most stable anchoring mode is the dissociative bridging bidentate one.<sup>27-31</sup> For Ru-based sensitizers, having generally two or more anchoring sites, different configurations are possible, essentially depending on the geometry of the complex. Also in this case the preferred adsorption geometry seems to be the bridging bidentate one, sometimes coexisting with the deprotonated monodentate.<sup>32-38</sup>

Concerning the stability in device working conditions (1Sun light soaking, T>50°C, variable moisture rate) it has been observed that, for a correctly assembled and sealed DSC, it mainly depends on the degradation and/or desorption of the sensitizer in the electrolyte solution. These issues dramatically affect the photocurrent production.<sup>39-41</sup> The electrolyte composition, obviously, can play a fundamental role in the degradation pathways at the dye/semiconductor interface. In particular, for ruthenium based dyes containing NCS ligands, the thiocyanate substitution with the 4-tertbutylpyridine additive or with nitrile based solvent molecules has been observed, leading to significant performance reductions.<sup>42-44</sup> On the other hand it has to be highlighted that this reaction takes place at significant rates only at elevated temperature (80-100°C). Furthermore, solvent molecules can introduce important modifications to the dye adsorption geometry, affecting the stability of the interaction, and potentially leading to dye desorption.<sup>45, 46</sup>

In the present study we report an investigation, through a joint experimental and theoretical approach, on the stability of devices sensitized with the black dye and Y1 coadsorbent, (Scheme 1) as reported in the work by Han and coworkers.<sup>19</sup> DSC devices have been subjected to enduring 1Sun illumination, at 55°C. The photoconversion efficiencies have been measured on the fresh and aged devices, after 300 and 1100h of light soaking. As a first approximation of the reasons for the performance degradation, the stability of the dyes anchoring on a TiO<sub>2</sub> surface has been theoretically investigated.

Our results show the realized devices maintain a significant stability under the investigated conditions. The slight decrement of the overall efficiency, due to the photocurrent reduction, could be attributed to the desorption of the organic dye, due a weaker interaction at the TiO<sub>2</sub> interface upon photoexcitation and during charge injection processes.

## 2 Experimental section

### 2.1 Materials and preparation of solar cells

All chemicals used in this work were stored in a dry room (relative humidity ~5%) and used without any further purification. All materials were purchased from either Dyesol or Sigma-Aldrich.

TCO sheet glass electrodes (Dyesol TEC15 2.3 mm, 15 Ω/sq) were used as substrates for nanocrystalline TiO<sub>2</sub> films. A thin TiO<sub>2</sub> underlayer (blocking layer) was deposited by immersing the TCO/glass substrate in a TiCl<sub>4</sub> aqueous solution for 30 min at 70 °C and then sintered at 500 °C for 1 hour. Mesoporous TiO<sub>2</sub> thin films (~15 μm thickness, 0.88 cm<sup>2</sup>) were deposited onto the conducting glass by screen-printing using Dyesol 18NR-AO TiO<sub>2</sub> paste and then sintered at 500 °C for 1 hour. The films' thickness was measured with a DEKTAK 150 surface profiler (Veeco Instruments Inc.). The dye solutions used were either a solution of black dye (Dyesol) or co-adsorbent Y1, synthesized according to the procedure reported in the original paper,<sup>19</sup> at 0.2 mM concentration, in dry ethanol or a mixture of both at a 1:1 ratio. The nanoporous TiO<sub>2</sub> films were immersed in the above solutions at 25 °C for 24 hours. The working and the counter-electrodes (platinum-coated conducting glass, Dyesol) were separated by an 80 μm thick Bynel® spacer and sealed by heating the polymer frame. Dyesol EL-HSE iodine-based high stability electrolyte, using 3-methoxypropionitrile (MPN) solvent was inserted via vacuum backfilling into the cells, and patches of thermoplastic material and glass used to close the fill hole. The devices were secondary sealed by Dyesol two part thermal cure epoxy compound.

## 2.2 Methods

The UV–Vis absorption spectra were recorded in acetonitrile (ACN) solution on a Perkin–Elmer Lambda 800 spectrophotometer.

Cell performance was evaluated by recording photocurrent density - photovoltage (J-V) characteristics and by Incident Photon to Current Efficiency (IPCE). J-V characteristics of DSCs were recorded via computer controlled digital source meter (Keithley 2420) using a 150 W metal halide lamp, which was calibrated by a silicon reference cell and corrected for any spectral mismatch on a clear day under full sun outdoor illumination (close to AM 1.5). In order to collect data at various light levels, incident light intensities were adjusted with wire mesh attenuators. IPCE was determined using a Pecell PEC-S20 Action Spectrum Measurement System in DC mode. Calibration was undertaken by a silicon photodiode model S1337-1010BQ.

Long-term light soaking was undertaken under the light of a metal halide lamp at ~1 Sun, where cell temperature was constantly maintained at ~55 °C. All cells were maintained close to their maximum power point by a resistive load during long-term testing.

## 2.3 Computational details

All the calculations were performed by DFT, as implemented in the Gaussian09 program suite.<sup>47</sup> Ground state geometry optimizations were obtained using the B3LYP hybrid functional<sup>48</sup> along with 6-31G\* basis set,<sup>49</sup> in acetonitrile solution. Solvent effects (ACN) were included using the Conductor-like Polarization Model, CPCM solvation model.<sup>50</sup>

To model the dye/TiO<sub>2</sub> interface, we used a neutral stoichiometric (TiO<sub>2</sub>)<sub>38</sub> cluster,<sup>51–53</sup> obtained by appropriately “cutting” an anatase slab exposing the majority (101) surface.<sup>54</sup> To model Y1 and Y2 organic dye@TiO<sub>2</sub> complexes, the most accepted bidentate bridging mode has been used.<sup>27</sup> N749@TiO<sub>2</sub> complex was modelled through dissociated monodentate binding, involving two carboxylic groups.<sup>55, 56</sup> Initial conformations for ACN and MPN on TiO<sub>2</sub> were modelled by keeping ~2.0 Å distance between surface Ti-atoms and N-atom of the solvent molecule. Equilibrium geometries in ACN solution for these complexes were obtained using the B3LYP functional and a 6-31G\* basis set for all atoms except Ruthenium, for which a DZVP basis set was used.

Adsorption energies ( $\Delta E_{\text{ads}}$ ) of dyes adsorbed on the TiO<sub>2</sub> surface were calculated from optimized geometries in solution, according to  $\Delta E_{\text{ads}} = E_{\text{Com}} - (E_{\text{Dye}^-} + E_{\text{TiO}_2\text{-H}^+})$  equation.  $E_{\text{Com}}$  is the total energy of dye@TiO<sub>2</sub> complex,  $E_{\text{Dye}^-}$  is the energy of deprotonated dye, as adsorbed on TiO<sub>2</sub> surface, and  $E_{\text{TiO}_2\text{-H}^+}$  is the energy of TiO<sub>2</sub> surface with the dissociate proton from the dye. Energies for deprotonated dye, and protonated TiO<sub>2</sub> fragments at the complex geometry were calculated by single point calculation in ACN solution using same level of theory employed for the complexes.

## 3 Results and discussion

### 3.1 Experimental Results

In order to differentiate the effect of each sensitizer on the overall stability of the solar cells we fabricated three kinds of devices: the first using only Y1 organic sensitizer, the second using N749 dye and the last employing a cocktail of both sensitizers (Table 1). Compared to the utilization of individual Y1 and N749 dyes, co-sensitization with N749-Y1 resulted in much higher efficiencies: 2.71, 4.94 and 5.75% respectively (Table 1). The obtained efficiencies are considerably lower than in the original paper,<sup>19</sup> reasonably due to the thinner TiO<sub>2</sub> films (15 vs. 25 μm), larger active area (0.88 vs. 0.25 cm<sup>2</sup>) and high stability electrolyte. Our electrolyte employs 3-methoxypropionitrile as solvent. It has a higher boiling point (164–165°C) compared to acetonitrile (81–82°C), but has been demonstrated to be less performing.<sup>57–59</sup>

**Table 1.** Photovoltaic parameters (assessed at 1/3 Sun) for DSC devices. Measurements on fresh and aged (~1 Sun light soaking, ~55 °C) are reported. Percentage difference ( $\Delta$ ) on the measured parameters compared to the fresh devices are also reported.

Dye	Time	J <sub>sc</sub> (mA/cm <sup>2</sup> )	V <sub>oc</sub> (mV)	FF	η (%)
Y1	0h	2.41	557	0.67	2.71
	300h	2.45	561	0.66	2.73
	Δ	+1.3%	+0.7%	-0.9%	+1.0%
	1100h	2.12	510	0.68	2.19
	Δ	-12.3%	-8.9%	+1.1%	-19.3%
N749	0h	5.19	565	0.56	4.94
	300h	5.11	609	0.56	5.28
	Δ	-1.6%	+7.9%	+0.5%	+6.8%
	1100h	5.08	590	0.58	5.23
	Δ	-2.0%	+5.0%	+2.7%	+5.8%
N749+Y1	0h	5.62	599	0.57	5.75
	300h	5.33	636	0.59	5.98
	Δ	-5.1%	+6.1%	+3.2%	+3.9%
	1100h	5.26	610	0.60	5.74
	Δ	-6.5%	+1.5%	+5.1%	-0.3%

By using the co-sensitization approach we obtain an increase in the  $J_{sc}$  values, compared to the isolated N749 based device, consistent with the increase in the light harvesting capability in the blue region (350-500nm) of the solar spectrum (Figure 1). This is readily converted in a gain in the IPCE in the same spectral region (see Electronic Supplementary Information, ESI).

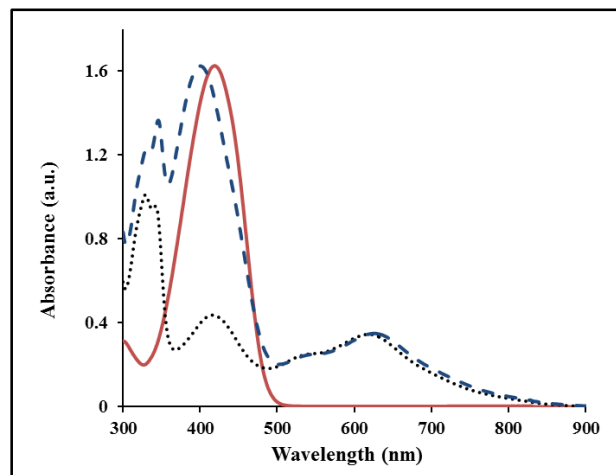


**Figure 1.** Absorbance spectra of Y1 (red line) N749 (dotted black line) and equimolar N749-Y1 dye mixture (dashed blue line) in acetonitrile solution.

Also in the  $V_{oc}$  values we can observe a significant increase ( $\sim 30$  mV), mainly due to the shielding effect of the Y1 coadsorbent on the  $TiO_2$  surface, effectively suppressing recombination processes and enhancing the electron lifetimes.<sup>19</sup> A key role in this regard is played by the butoxyl chains on the donor part of the molecule, that are able to keep the oxidized  $I_3^-$  ions far from the semiconductor surface, and to efficiently act as an antiaggregation agent.<sup>60</sup> Despite the lower efficiencies the trend of the measured parameters are however consistent with the original paper.<sup>19</sup>

Stability of the investigated devices was assessed with J-V measurements at  $\frac{1}{3}$  Sun. The results are presented in Table 1 and Figure 2.

After 300h light soaking, all devices remain stable. We observe slight increases in the performances ( $\sim 1\%$  for Y1, 4% for Y1+N749 and 7% for N749), mostly due to a slight increase in  $V_{oc}$ . After 1100h, the N749-sensitized device still remains stable, in line with previous investigation of ruthenium dyes in similar testing conditions.<sup>57, 61, 62</sup> The organic Y1 dye shows instead a substantial drop with respect to the initial efficiency ( $-19.3\%$ ), due to a parallel reduction of both  $J_{sc}$  and  $V_{oc}$ . For the device employing the N749-Y1 dyes cocktail, we observe an intermediate behaviour, with a negligible efficiency decrease, suggesting that the device's performances slightly suffers from the lower long term stability of the Y1 co-adsorbent, compared to N749.

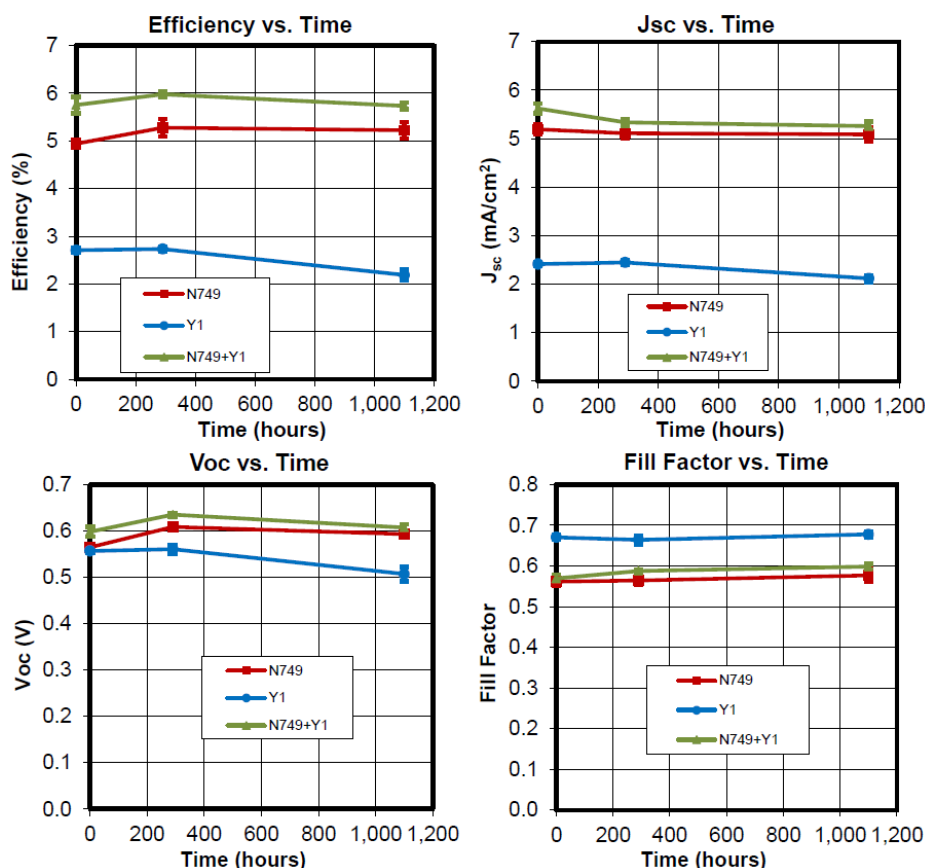


**Figure 2.** Stability of the photovoltaic parameters during ageing tests (300 h and 1100 h under  $\sim 1$  Sun light soaking and  $\sim 55^\circ C$ ). Measurements were made at  $\frac{1}{3}$  Sun illumination.

### 3.2 Theoretical calculations

As pointed out in the introduction, one of the main causes for the lack of long term stability, resides in the dye degradation or desorption. To shed light on the different stability between the two dyes, a computational investigation on the adsorption geometries and energies on an anatase  $\text{TiO}_2$  cluster has been carried out. Our aim is to understand if there could be a correlation between the adsorption behaviour of the sensitizers and their long term stability in the DSC devices. In order to simulate the stability of the neutral and oxidized dyes, the latter occurring after charge injection process, we modelled the dyes in their neutral form and after removing one electron.

We simulated the N749 and Y1 dyes, and then extended our analysis to the Y2 co-adsorbent, used in the original work with

slightly lower performances<sup>19</sup> (Scheme 1). To assess the competition for solvent molecules to bind the undercoordinated  $\text{TiO}_2$  sites, we also simulated adsorption of acetonitrile ACN and MPN molecules, since these are the most commonly employed solvents in liquid electrolyte solar cells. Concerning N749 dye, that is an anionic complex,<sup>63</sup> we modelled two forms: the anionic one, and the neutral one, considering one tetrabutylammonium counterion (TBA). It has been placed near to the thiocyanate ligands, where a partial negative charge is majorly localized. The optimized geometries for all the considered systems are reported in Figure 3.

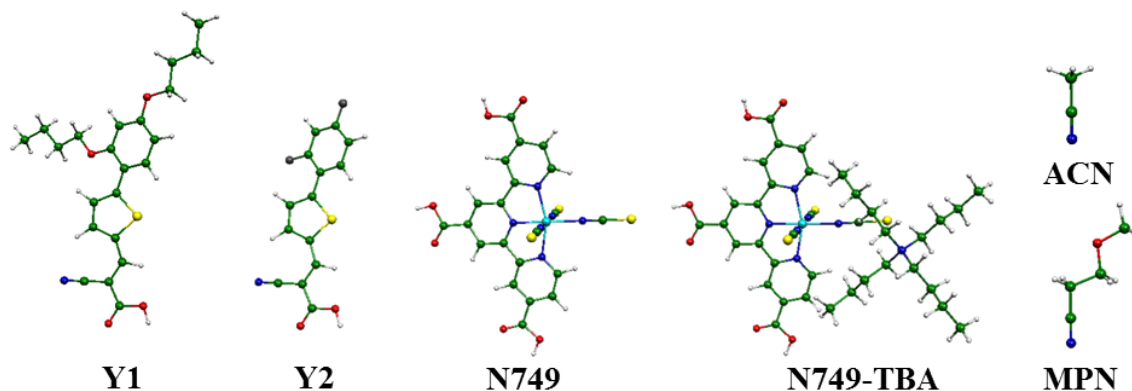


**Figure 3.** Optimized geometries of Y1, Y2, N749 dye, [N749-TBA], acetonitrile (ACN) and 3-methoxypropionitrile (MPN).

**Organic co-adsorbent dyes** The optimized Y1 and Y2 dyes exhibit quite planar geometries, except for a dihedral angle of  $24^\circ$  between the phenyl and the thiophene planes (Figure 3). This distortion from planarity does not prevent the conjugation extension over the whole donor- $\pi$  spacer-acceptor (D- $\pi$ -A) molecular structure, as recently observed by Azar and Payami.<sup>60</sup> This is clearly visible from the HOMO-LUMO plot of the Y1 and Y2 dyes (Figure 4).

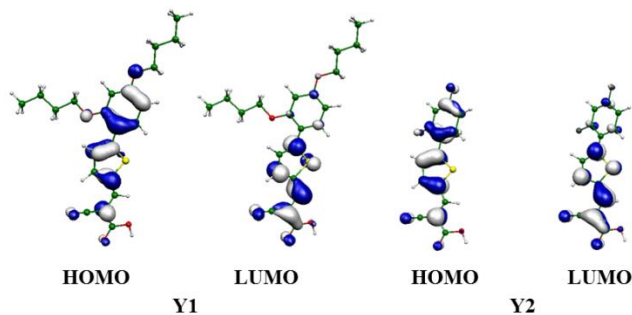


**Figure 4.** HOMO-LUMO isodensity plot of Y1 and Y2 dyes.

Similarly to related push-pull sensitizers the HOMO is localized on the donor and  $\pi$ -bridge moieties, while the LUMO is mainly located over the cyanoacrylic acceptor group. The

high overlap between the HOMO and LUMO molecular orbitals, being mainly involved in the lowest energy transition, may account for the high molar extinction coefficients measured for the two dyes ( $3.0 \times 10^4 \text{ M}^{-1} \text{ cm}^{-1}$  and  $3.1 \times 10^4 \text{ M}^{-1} \text{ cm}^{-1}$ , for Y1 and Y2, respectively).<sup>19</sup>

Moving to the optimization of the oxidized Y1 and Y2 dyes (Figure 5) we note a slight reorganization of both the molecules. In particular we calculate the planarization of the dye structures, in conjunction with a reduction of the C-C bond between the phenyl and the thiophene ring (from 1.46 to 1.42 Å for both molecules). Analysis of the spin density plots (Figure 5) for  $\text{Y1}^{\text{ox}}$  shows that the hole is highly delocalised along all the dye backbone. For  $\text{Y2}^{\text{ox}}$  dye, hole is instead mainly localized on two carbon atoms on the spacer and the acceptor part of the molecule, with a significant contribution also on the cyanoacrylic moiety. This different behaviour between the two molecules may be due to the different substituents on the donor part of the molecules. The electron donating effect of the alkoxy groups for Y1 is probably able to better stabilize the positive charge on the oxidized structure. The higher localization of the hole in the acceptor region of the Y2 dye molecule may account for the slight lower photovoltaic performances compared to Y1,<sup>19</sup> due to an increase of the

## ARTICLE

recombination probability of the injected electrons with the oxidized dye.

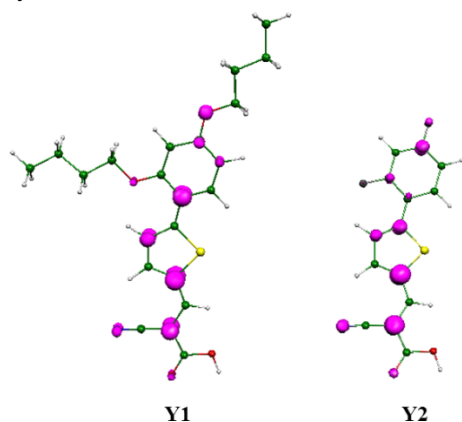


**Figure 5.** Spin density plots (purple surface) for the oxidized Y1 and Y2 dyes.

To simulate the dye adsorption onto the  $\text{TiO}_2$  anatase (101) surface, dye molecules were chemisorbed using a dissociative bridging bidentate anchoring mode, as proposed in our previous works.<sup>27, 64</sup> The two oxygen atoms of the  $\text{COO}^-$  anchor were bound to five coordinated titanium atoms, while the acidic proton was bound to a vicinal oxygen atom. Equilibrium geometries of these complexes are reported in Figure 6 (a and b), while main geometrical parameters for dye- $\text{TiO}_2$  interfaces are provided in the ESI.

Both dyes show a quite strong interaction with the semiconductor surface, with short bond distances (within 2.0 and 2.2 Å) between the carboxylic oxygen and the coordinating titanium atoms. Further inspection of the optimized structures reveals that the dye geometry does not show substantial changes upon the adsorption on the semiconductor. We then moved to the simulation of the Y1 cation adsorbed on the  $\text{TiO}_2$  surface. Interestingly, compared to the neutral dye@ $\text{TiO}_2$  complex, we can note a partial elongation ( $\sim 0.05$  Å) of both the Ti-O bonds of the anchoring, suggesting a slightly less stable interaction between the dye and the semiconductor surface, upon oxidation. Inspection of the spin density plot of  $\text{Y1}^{\text{ox}}@ \text{TiO}_2$  (see ESI) reveals again an efficient delocalization of the hole along the whole dye backbone, as found for the isolated dye in solution. The delocalization of the hole justifies the just slight changes in the anchoring geometry. Further inspection of the complex structure highlights the same reorganization of the molecular structure observed for the dye in solution, with a planarization of the phenyl and thiophene dihedral angle.

**N749 in solution and adsorbed on  $\text{TiO}_2$**  The same computational procedure has been carried out for the fully protonated N749 ruthenium dye. Optimized geometries are reported in Figure 3 and in Figure 7 (for oxidized compounds).

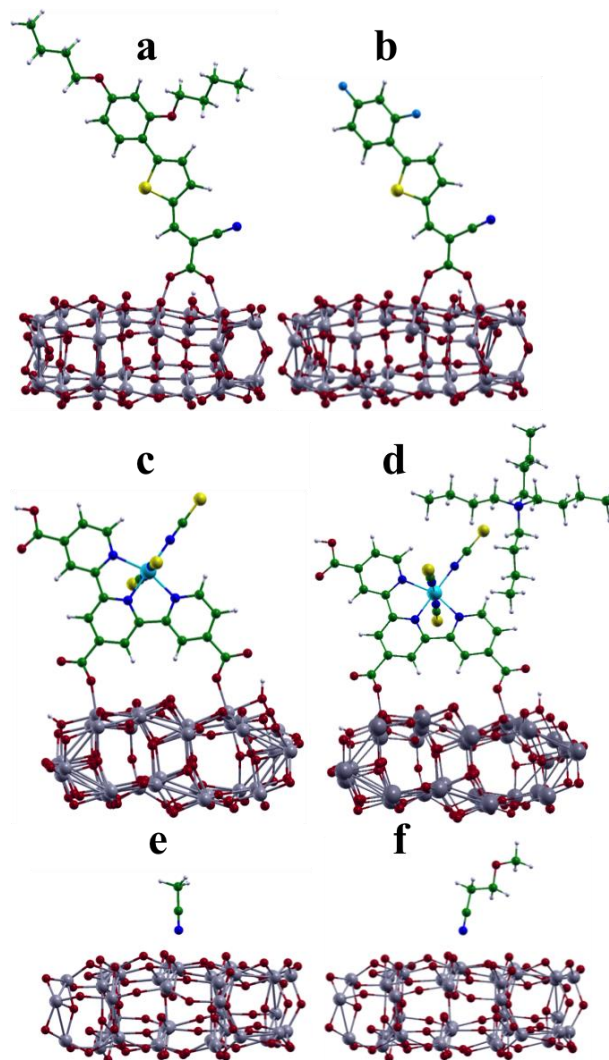


**Figure 6.** Optimized geometries of (a)  $\text{Y1}@ \text{TiO}_2$ , (b)  $\text{Y2}@ \text{TiO}_2$ , (c)  $\text{N749}@ \text{TiO}_2$ , (d)  $[\text{N749-TBA}]@ \text{TiO}_2$ , (e)  $\text{ACN}@ \text{TiO}_2$  and (f)  $\text{MPN}@ \text{TiO}_2$ .

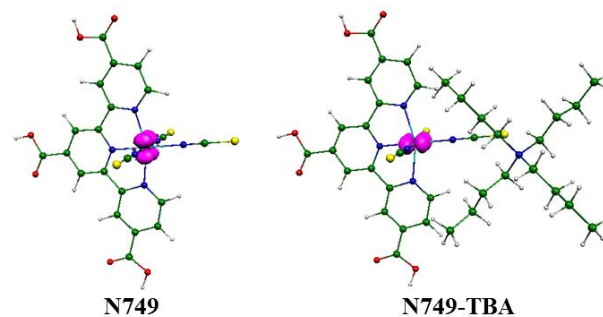


**Figure 7.** Spin density plots (purple surface) for oxidized N749 and N749-TBA systems.

In the Figure 7, concerning the oxidized complexes, the spin density plots are also represented. The hole is highly localized on the metal centre for both systems. The main geometrical

variations upon oxidation of the complexes relate to the Ru-N bonds, that are generally contracted by  $\sim 0.06$  Å, due to the need to stabilize the hole. Essentially no effect on the terpyridine ligand, bearing the anchoring carboxylic groups, is observed. It is worth noting that for N749 dye the hole is localized away from anchor, contrary to Y1 and Y2 dye. This is an important factor to retard electron-hole recombination and can be highlighted as one of the reasons for impressive photovoltaic performance of N749 dye.

The adsorption geometry of N749 dye on TiO<sub>2</sub> has been deeply investigated in the last years. Experimentally, Bauer et al., in 2002, suggested a bidentate binuclear coordination, on the basis of FT-IR investigation.<sup>65</sup> From the theoretical side different results have been obtained depending on the employed computational approach.<sup>55, 56, 66-69</sup> In a recent work from our group, anchoring through two dissociated monodentate carboxylic groups resulted the most stable one,<sup>55, 56</sup> similarly to what was found for heteroleptic ruthenium dyes.<sup>70</sup> Very recently Tateyama et al. through molecular dynamics studies confirmed this binding mode as the most favoured, whereas the single anchoring through protonated carboxylic acid could be present to a less extent.<sup>69</sup>

Here we just focus on the most stable adsorption mode, through two dissociated monodentate carboxylic groups (Figure 6, *c* and *d*). As expected, a strong interaction between dye and TiO<sub>2</sub> surface is found, with Ti-O bond distances of less than 2 Å. A strong contribution to the stabilization of the anchoring is given by the hydrogen bond formation between the carboxylate oxygen and the protons transferred to the TiO<sub>2</sub> surface. This is also suggested by the fact that presence of protic solvents, such as water, reduce the stability of the anchoring.<sup>45, 71</sup> Noteworthy the best results in terms of device stability has been obtained with amphiphilic dyes, such as Z907, able to effectively insulate the dye/semiconductor interface from the approach of water.<sup>72</sup>

Optimized geometries for the oxidized N749@TiO<sub>2</sub> complexes show just marginal or no difference in adsorption bond lengths between carboxylate oxygen and surface titanium atoms. Similarly to the case of isolated N749 in solution, we can see from the spin density plot as in the oxidized complex the hole is completely localized on the ruthenium centre, thus having a negligible effect on the terpyridine ligand and on the carboxylic groups. A detailed list of the geometrical parameters for the different investigated species is reported in the ESI.

**ACN and MPN solvent molecules** Optimized geometries for ACN and MPN solvents are given in Figure 2. To understand the behaviour of these solvents at the TiO<sub>2</sub> interface, one molecule of ACN and MPN electrolyte solvent was adsorbed at a five-fold coordinated Ti atom of the surface (Figure 6, *e* and *f*). Both the solvents interact with the surface via nitrogen atom, and stabilize at a distance of 2.31 Å. In reasonable agreement with a previous investigation, we find a “standing” structure for the solvent adsorbed molecules, with angles between Ti, N and C atoms (of the nitrile groups) of  $\sim 170^\circ$ .<sup>73</sup>

**Adsorption energies** Calculated adsorption energies for the investigated complexes are given in Table 4. The results show a comparable binding between the organic Y1 and the Y2 dyes (-71.1 kcal/mol and -69.3 kcal/mol respectively). N749 dye, in both the anionic form and the neutral one, with the TBA counterion, has a much stronger adsorption, with energies of about -120 kcal/mol. The large difference between binding energies of Y1/Y2 and N749 dyes are easily expected by observing their different adsorption geometries (Figure 6). Here, Y1 and Y2 dyes anchor with one COO<sup>-</sup> group on TiO<sub>2</sub>, whereas N749 dye adsorbs using two COO<sup>-</sup> moieties. As previously shown, further stabilization of the black dye adducts comes from hydrogen bond formation between the carboxylate oxygen atoms and the dissociated hydrogen atoms on the TiO<sub>2</sub> surface. Obviously, the electrolyte solvents show considerably lower adsorption energies, of almost one order of magnitude, with respect to the sensitizing dyes, having a negligible competition for the semiconductor binding sites.

**Table 2.** Adsorption energies of the investigated compounds on anatase (101) TiO<sub>2</sub> surface.

Dye@TiO <sub>2</sub>	$\Delta E_{\text{ads}}$ (kcal/mol)
Y1	-71.1
Y1 <sup>ox</sup>	-58.9
Y2	-69.3
N749	-118.0
[N749] <sup>ox</sup>	-110.1
[N749-TBA]	-121.3
[N749-TBA] <sup>ox</sup>	-120.4
Solvent@TiO <sub>2</sub>	$\Delta E_{\text{ads}}$ (kcal/mol)
ACN	-13.8
MPN	-8.5

Interestingly, the higher adsorption energy for N749 dye suggests a stronger tendency to graft on the surface during the sensitization process. At the same concentration of the dye bath solution for Y1 and N749 dyes, as reported in the experimental details, the ruthenium dye is probably preferably adsorbed, while the small organic dye could fill the remaining binding sites. This can explain the improved photovoltaic performances of the device sensitized with the dye cocktail, since the presence of Y1 dye does not limit the adsorption of the more efficient black dye. The light absorption and charge transfer properties of Y1 has instead an additive effect on the overall conversion efficiency of the co-sensitized devices. This assumption is also coherent with the degradation behaviour of the DSC devices. The cells sensitized with the mixture of both dyes, in fact, show just a slight decrease of the efficiency upon light soaking (-0.3%), similarly to the stability behaviour of the individual N749 dye.

Charge transfer from photo-excited dye to TiO<sub>2</sub> conduction band results in the localization of hole on oxidized dye. The temporarily formed electron deficient donor can weaken the interaction between adsorbed dye and TiO<sub>2</sub>, by drawing electron density from the anchor moiety. Therefore, it is important to look also at the adsorption energies for the oxidized dye@TiO<sub>2</sub> complexes. Our results show an adsorption energy for the oxidized Y1<sup>ox</sup>@TiO<sub>2</sub> complex of -58.9 kcal/mol, which is considerably lower (-17%) compared to the neutral system. On the other hand, oxidized N749@TiO<sub>2</sub> complexes present a negligible reduction in binding energies (-6.7%, or -1%, depending on the employed model). As previously shown, for the ruthenium dye the hole is strongly localized on the metal centre, with negligible effect on the terpyridine ligand and on the carboxylic anchoring groups, reflecting the just slight reduction in the adsorption energy. For Y1 dye, the hole delocalizes along the dye structure, showing a partial lengthening of the anchoring bond distances and a consistent reduction of the adsorption energy.

This data suggest the desorption of Y1 dye, in particular upon oxidation, as one of the possible main causes of the observed lower long term stability for the measured devices under light soaking and thermal stressing conditions, compared to N749 black dye. Noteworthy the drop of conversion efficiency for Y1-sensitized devices is mainly due to photocurrent reduction, consistently with previous papers investigating dye desorption.<sup>39, 40</sup> Significant improvements in the long-term durability for organic dyes have been obtained when di-anchoring sensitizer have been used,<sup>74, 75</sup> suggesting that the stability of dye/semiconductor interaction is a key point in order to develop efficient and robust dyes for DSCs applications.

## Conclusions

We have investigated the stability of DSC devices employing black dye and Y1 organic coadsorbent, under light soaking for 1100h at 1 sun, at 55°C. Our study showed a remarkable stability of the devices employing N749 sensitizer or the dye cocktail, while a 20% reduction in the photovoltaic efficiency has been measured for the isolated Y1 organic dye. A theoretical investigation on the adsorption energies and geometries of the considered sensitizers on an anatase TiO<sub>2</sub> cluster has been carried out in order to evaluate the stability of the dye anchoring as a possible cause of the performance degradation. Consistently with the experimental results we found a considerably higher adsorption energy for the N749 dye, due to the double carboxylic anchoring, with respect to the Y1 dye. Noteworthy, the latter has also shown a significant reduction of the binding energy upon oxidation, suggesting possible dye desorption as a reliable explanation for the lower stability under stress conditions.

## Acknowledgements

The authors are thankful to the joint DST-EU project 'ESCORT' (FP7-ENERGY-2010, contract 261920) for financial support of this work. MC thanks DST, New Delhi for funding the project No. DST/TMC/SERI/FR/92.

## Notes and references

<sup>a</sup> D3-Computation, Istituto Italiano di Tecnologia, Via Morego 30, I-16163 Genova, Italia. E-mail: [Paolo.Salvatori@iit.it](mailto:Paolo.Salvatori@iit.it), Phone: +39 075 585 5522, Fax: +39 075 585 5606.

<sup>b</sup> Computational Laboratory for Hybrid/Organic Photovoltaics (CLHYO), Istituto CNR di Scienze e Tecnologie Molecolari (ISTM-CNR), Via Elce di Sotto 8, I-06123, Perugia, Italia. E-mail: [filippo@thch.unipg.it](mailto:filippo@thch.unipg.it), Phone: +39 075 585 5522, Fax: +39 075 585 5606.

<sup>c</sup> CSIR-Indian Institute of Chemical Technology, Uppal Road, Tarnaka, Hyderabad-500 607, India.

<sup>d</sup> Dyesol UK Ltd. UMIC-Incubator Building, University of Manchester, 48 Grafton Street, M13 9XX, UK.

Electronic Supplementary Information (ESI) available: [IPCE graphics, detailed list of geometrical parameters for dyes and solvents adsorbed on TiO<sub>2</sub>, spin density plots for oxidized Y1 and N749 on TiO<sub>2</sub>]. See DOI: 10.1039/b000000x/

- 1 M. Grätzel, *Nature*, 2001, **414**, 338-344.
- 2 M. Grätzel, *Acc. Chem. Res.*, 2009, **42**, 1788-1798.
- 3 A. Hagfeldt, G. Boschloo, L. Sun, L. Kloo and H. Pettersson, *Chem. Rev.*, 2010, **110**, 6595-6663.
- 4 B. O'Regan and M. Grätzel, *Nature*, 1991, **353**, 737-740.
- 5 S. Mathew, A. Yella, P. Gao, R. Humphry-Baker, F. E. Curchod Basile, N. Ashari-Astani, I. Tavernelli, U. Rothlisberger, M. K. Nazeeruddin and M. Grätzel, *Nat. Chem.*, 2014, **6**, 242-247.
- 6 M. K. Nazeeruddin, A. Kay, I. Rodicio, R. Humphry-Baker, E. Mueller, P. Liska, N. Vlachopoulos and M. Grätzel, *J. Am. Chem. Soc.*, 1993, **115**, 6382-6390.
- 7 M. K. Nazeeruddin, P. Pechy and M. Grätzel, *Chem. Commun.*, 1997, **0**, 1705-1706.
- 8 P. G. Bomben, K. C. D. Robson, B. D. Koivisto and C. P. Berlinguette, *Coord. Chem. Rev.*, 2012, **256**, 1438-1450.
- 9 W. M. Campbell, A. K. Burrell, D. L. Officer and K. W. Jolley, *Coord. Chem. Rev.*, 2004, **248**, 1363-1379.
- 10 A. Kay and M. Grätzel, *J. Phys. Chem.*, 1993, **97**, 6272-6277.
- 11 L.-L. Li and E. W.-G. Diau, *Chem. Soc. Rev.*, 2013, **42**, 291-304.
- 12 S. Namuangruk, K. Sirithip, R. Rattanatwan, T. Keawin, N. Kungwan, T. Sudyodsuk, V. Promarak, Y. Surakhot and S. Jungstittiwong, *Dalton Trans.*, 2014, **43**, 9166-9176.
- 13 A. Mishra, M. K. R. Fischer and P. Bäuerle, *Angew. Chem. Int. Ed.*, 2009, **48**, 2474-2499.
- 14 M. Zhang, Y. Wang, M. Xu, W. Ma, R. Li and P. Wang, *Energy Environ. Sci.*, 2013, **6**, 2944-2949.
- 15 S.-Q. Fan, C. Kim, B. Fang, K.-X. Liao, G.-J. Yang, C.-J. Li, J.-J. Kim and J. Ko, *J. Phys. Chem. C*, 2011, **115**, 7747-7754.
- 16 L. H. Nguyen, H. K. Mulmudi, D. Sabba, S. A. Kulkarni, S. K. Batabyal, K. Nonomura, M. Grätzel and S. G. Mhaisalkar, *Phys. Chem. Chem. Phys.*, 2012, **14**, 16182-16186.

- 17 J.-H. Yum, E. Baranoff, S. Wenger, M. K. Nazeeruddin and M. Grätzel, *Energy Environ. Sci.*, 2011, **4**, 842-857.
- 18 A. Yella, H.-W. Lee, H. N. Tsao, C. Yi, A. K. Chandiran, M. K. Nazeeruddin, E. W.-G. Diao, C.-Y. Yeh, S. M. Zakeeruddin and M. Grätzel, *Science*, 2011, **334**, 629-634.
- 19 L. Han, A. Islam, H. Chen, C. Malapaka, B. Chiranjeevi, S. Zhang, X. Yang and M. Yanagida, *Energy Environ. Sci.*, 2012, **5**, 6057-6060.
- 20 G. Boschloo and A. Hagfeldt, *Acc. Chem. Res.*, 2009, **42**, 1819-1826.
- 21 P. Persson, M. J. Lundqvist, R. Ernstorfer, W. A. Goddard and F. Willig, *J. Chem. Theory Comput.*, 2006, **2**, 441-451.
- 22 M. J. Lundqvist, M. Nilsing, S. Lunell, B. Åkermark and P. Persson, *J. Phys. Chem. B*, 2006, **110**, 20513-20525.
- 23 J. Wiberg, T. Marinado, D. P. Hagberg, L. Sun, A. Hagfeldt and B. Albinsson, *J. Phys. Chem. C*, 2009, **113**, 3881-3886.
- 24 M. Pastore and F. De Angelis, *Phys. Chem. Chem. Phys.*, 2012, **14**, 920-928.
- 25 F. Odobel, E. Blart, M. Lagree, M. Villieras, H. Boujtitia, N. El Murr, S. Caramori and C. Alberto Bignozzi, *J. Mater. Chem.*, 2003, **13**, 502-510.
- 26 A. Abbotto, N. Manfredi, C. Marini, F. De Angelis, E. Mosconi, J.-H. Yum, Z. Xianxi, M. K. Nazeeruddin and M. Grätzel, *Energy Environ. Sci.*, 2009, **2**, 1094-1101.
- 27 C. Anselmi, E. Mosconi, M. Pastore, E. Ronca and F. De Angelis, *Phys. Chem. Chem. Phys.*, 2012, **14**, 15963-15974.
- 28 M. Pastore and F. De Angelis, *ACS Nano*, 2010, **4**, 556-562.
- 29 H. Tian, X. Yang, R. Chen, R. Zhang, A. Hagfeldt and L. Sun, *J. Phys. Chem. C*, 2008, **112**, 11023-11033.
- 30 P. Chen, J. H. Yum, F. De Angelis, E. Mosconi, S. Fantacci, S.-J. Moon, R. H. Baker, J. Ko, M. K. Nazeeruddin and M. Grätzel, *Nano Letters*, 2009, **9**, 2487-2492.
- 31 W. H. Howie, F. Claeysens, H. Miura and L. M. Peter, *J. Am. Chem. Soc.*, 2008, **130**, 1367-1375.
- 32 M. K. Nazeeruddin, R. Humphry-Baker, P. Liska and M. Grätzel, *J. Phys. Chem. B*, 2003, **107**, 8981-8987.
- 33 P. Falaras, *Sol. Energy Mater. Sol. Cells*, 1998, **53**, 163-175.
- 34 C. Pérez León, L. Kador, B. Peng and M. Thelakkat, *J. Phys. Chem. B*, 2006, **110**, 8723-8730.
- 35 T. Moehl, H. N. Tsao, K.-L. Wu, H.-C. Hsu, Y. Chi, E. Ronca, F. De Angelis, M. K. Nazeeruddin and M. Grätzel, *Chem. Mater.*, 2013, **25**, 4497-4502.
- 36 F. De Angelis, S. Fantacci, A. Selloni, M. Grätzel and M. K. Nazeeruddin, *Nano Lett.*, 2007, **7**, 3189-3195.
- 37 K. S. Finnie, J. R. Bartlett and J. L. Woolfrey, *Langmuir*, 1998, **14**, 2744-2749.
- 38 F. Schiffmann, J. VandeVondele, J. r. Hutter, R. Wirz, A. Urakawa and A. Baiker, *J. Phys. Chem. C*, 2010, **114**, 8398-8404.
- 39 A. Hinsch, J. M. Kroon, R. Kern, I. Uhlendorf, J. Holzbock, A. Meyer and J. Ferber, *Progr. Photovolt. Res. Appl.*, 2001, **9**, 425-438.
- 40 P. M. Sommeling, M. Späth, H. J. P. Smit, N. J. Bakker and J. M. Kroon, *J. Photochem. Photobiol. A*, 2004, **164**, 137-144.
- 41 M. I. Asghar, K. Miettunen, J. Halme, P. Vahermaa, M. Toivola, K. Aitola and P. Lund, *Energy Environ. Sci.*, 2010, **3**, 418-426.
- 42 A. R. Andersen, J. Halme, T. Lund, M. I. Asghar, P. T. Nguyen, K. Miettunen, E. Kemppainen and O. Albrektsen, *J. Phys. Chem. C*, 2011, **115**, 15598-15606.
- 43 H. T. Nguyen, H. M. Ta and T. Lund, *Sol. Energy Mater. Sol. Cells*, 2007, **91**, 1934-1942.
- 44 P. T. Nguyen, R. Degn, H. T. Nguyen and T. Lund, *Sol. Energy Mater. Sol. Cells*, 2009, **93**, 1939-1945.
- 45 E. Mosconi, A. Selloni and F. De Angelis, *J. Phys. Chem. C*, 2012, **116**, 5932-5940.
- 46 A. F. Bartelt, R. Schütz, C. Strothkämper, I. Kastl, S. Janzen, D. Friedrich, W. Calvet, G. Fuhrmann, D. Danner, L.-P. Scheller, G. Nelles and R. Eichberger, *Appl. Phys. Lett.*, 2014, **104**, -.
- 47
- 48 A. D. Becke, *J. Chem. Phys.*, 1993, **98**, 1372-1377.
- 49 G. A. Petersson and M. A. Al-Laham, *J. Chem. Phys.*, 1991, **94**, 6081-6090.
- 50 M. Cossi and V. Barone, *J. Chem. Phys.*, 2001, **115**, 4708-4717.
- 51 M. J. Lundqvist, M. Nilsing, P. Persson and S. Lunell, *Int. J. Quantum Chem.*, 2006, **106**, 3214-3234.
- 52 F. De Angelis, A. Tilocca and A. Selloni, *J. Am. Chem. Soc.*, 2004, **126**, 15024-15025.
- 53 P. Persson, R. Bergström and S. Lunell, *J. Phys. Chem. B*, 2000, **104**, 10348-10351.
- 54 A. Vittadini, A. Selloni, F. P. Rotzinger and M. Grätzel, *Phys. Rev. Lett.*, 1998, **81**, 2954-2957.
- 55 S. Fantacci, M. G. Lobello and F. De Angelis, *CHIMIA* 2013, **67**, 121-128.
- 56 A. R. Srimath Kandada, S. Fantacci, S. Guarnera, D. Polli, G. Lanzani, F. De Angelis and A. Petrozza, *ACS Appl. Mater. Interfaces*, 2013, **5**, 4334-4339.
- 57 D. Kuang, C. Klein, S. Ito, J. E. Moser, R. Humphry-Baker, N. Evans, F. Durrant, C. Grätzel, S. M. Zakeeruddin and M. Grätzel, *Adv. Mater.*, 2007, **19**, 1133-1137.
- 58 A. Fukui, R. Komiya, R. Yamanaka, A. Islam and L. Han, *Sol. Energy Mater. Sol. Cells*, 2006, **90**, 649-658.
- 59 R. Katoh, M. Kasuya, A. Furube, N. Fuke, N. Koide and L. Han, *Sol. Energy Mater. Sol. Cells*, 2009, **93**, 698-703.
- 60 Y. T. Azar and M. Payami, *Phys. Chem. Chem. Phys.*, 2014, **16**, 9499-9508.
- 61 R. Harikisun and H. Desilvestro, *Solar Energy*, 2011, **85**, 1179-1188.
- 62 D. Shi, N. Pootrakulchote, R. Li, J. Guo, Y. Wang, S. M. Zakeeruddin, M. Grätzel and P. Wang, *J. Phys. Chem. C*, 2008, **112**, 17046-17050.
- 63 M. K. Nazeeruddin, P. Pèchy, T. Renouard, S. M. Zakeeruddin, R. Humphry-Baker, P. Comte, P. Liska, L. Cevey, E. Costa, V. Shklover, L. Spiccia, G. B. Deacon, C. A. Bignozzi and M. Grätzel, *J. Am. Chem. Soc.*, 2001, **123**, 1613-1624.
- 64 M. Pastore and F. De Angelis, *J. Phys. Chem. Lett.*, 2012, **3**, 2146-2153.
- 65 C. Bauer, G. Boschloo, E. Mukhtar and A. Hagfeldt, *J. Phys. Chem. B*, 2002, **106**, 12693-12704.
- 66 J. Chen, F.-Q. Bai, J. Wang, L. Hao, Z.-F. Xie, Q.-J. Pan and H.-X. Zhang, *Dyes and Pigments*, 2012, **94**, 459-468.
- 67 K. Sodeyama, M. Sumita, C. O'Rourke, U. Terranova, A. Islam, L. Han, D. R. Bowler and Y. Tateyama, *J. Phys. Chem. Lett.*, 2012, **3**, 472-477.
- 68 S.-H. Liu, H. Fu, Y.-M. Cheng, K.-L. Wu, S.-T. Ho, Y. Chi and P.-T. Chou, *J. Phys. Chem. C*, 2012, **116**, 16338-16345.

## ARTICLE

- 69 Y. Tateyama, M. Sumita, Y. Ootani, K. Aikawa, R. Jono, L. Han and K. Sodeyama, *J. Phys. Chem. C*, 2014,
- 70 F. De Angelis, G. Vitillaro, L. Kavan, M. K. Nazeeruddin and M. Grätzel, *J. Phys. Chem. C*, 2012, **116**, 18124-18131.
- 71 H. Pettersson and T. Gruszecki, *Sol. Energy Mater. Solar Cells*, 2001, **70**, 203-212.
- 72 P. Wang, S. M. Zakeeruddin, J. E. Moser, M. K. Nazeeruddin, T. Sekiguchi and M. Gratzel, *Nat. Mater.*, 2003, **2**, 402-407.
- 73 M. Sumita, K. Sodeyama, L. Han and Y. Tateyama, *The Journal of Physical Chemistry C*, 2011, **115**, 19849-19855.
- 74 A. Abboto, V. Leandri, N. Manfredi, F. De Angelis, M. Pastore, J.-H. Yum, M. K. Nazeeruddin and M. Grätzel, *Eur. J. Org. Chem.*, 2011, **2011**, 6195-6205.
- 75 X. Ren, S. Jiang, M. Cha, G. Zhou and Z.-S. Wang, *Chem. Mater.*, 2012, **24**, 3493-3499.